TIME-REVERSAL APERTURE ENHANCEMENT

J.-P. FOUQUE* AND K. SOLNA[†]

Abstract. Time-reversal refocusing for waves propagating in inhomogeneous media have recently been observed and studied experimentally in various contexts (ultrasound, underwater acoustics, ...), see for instance [9]. Important potential applications have been proposed in various fields, for instance in imaging or communication. However, the full mathematical analysis, meaning both modeling of the physical problem and derivation of the time-reversal effect is a deep and complex problem. Two cases that have been considered in depth recently corresponds to one dimensional media and the parabolic approximation regime where the backscattering is negligible. In this paper we give a complete analysis of time-reversal of waves emanating from a point source and propagating in a three dimensional randomly layered medium. The wave transmitted through the random medium is recorded on a small time-reversal mirror and sent back into the medium, time-reversed. Our analysis enables us to contrast the refocusing properties of a homogeneous medium and a random medium. We show that random medium fluctuations actually enhances the spatial refocusing around the initial source position. We consider a regime where the correlation length of the medium is much smaller than the pulse width, which itself is much smaller than the distance of propagation. We derive asymptotic formulas for the refocused pulse which we interpret in terms of an enhanced effective aperture. This interpretation is in fact comparable to the super-resolution effect obtained in the other extreme regime corresponding to the parabolic approximation. However, as we discuss, the mechanism that generates the super-resolution is very different in these two extreme situations.

1. Introduction.

In this paper we present a mathematical analysis of time-reversal in the case with waves propagating through randomly layered media. The one dimensional case where incoherent waves are time-reversed and sent back into the medium is well understood in the regime of separation of scales, we refer to [8, 10, 11, 12, 15, 19]. In this paper we discuss the three dimensional layered case where waves propagate from a point source. In Section 1.2 we describe in detail the physical problem that we will study, the time-reversal experiment for acoustic waves in three dimensional randomly layered media. We summarize the important separation of scales assumptions that we make in Section 1.3 following [1]. In Section 2 we derive an integral representation for the transmitted wave in terms of the transmission coefficients associated with the different wave modes. We briefly review in Section 3 the description of the transmitted coherent field, known as the O'Doherty-Anstey theory [17], studied in [6, 7, 13, 14, 16, 20]. Next, we describe the time-reversed and reflected wave and derive the super-resolution effect that enhances the refocusing obtained in a homogeneous medium which is constrained by the diffraction limit. Our precise analysis enables us to explain the mechanism which produces this enhanced aperture and how it differs from the one studied in the parabolic approximation regime in [4, 2, 18]. We discuss the comparison between these mechanisms in Section 5.

1.1. Acoustic waves.

We consider linear acoustic waves propagating in a three dimensional medium.

The equations for the **velocity u** and **pressure** p are:

$$(1.1) \qquad \rho\frac{\partial \mathbf{u}}{\partial t} + \nabla p = 0$$

$$\frac{1}{K}\frac{\partial p}{\partial t} + \nabla \cdot \mathbf{u} = 0$$

with ρ being the **density** and K the **bulk modulus.** These two equations correspond

respectively to conservation of momentum and mass. In the model problem that we consider the medium parameters are heterogeneous in the slab $0 < z < L$. We aim at describing waves propagating in a strongly heterogeneous medium like in the earth's crust. The fluctuations in the medium are then very complicated and we cannot expect to know them pointwise, however, we might be able to describe them statistically. Thus, we model the fluctuations of the medium in terms of a centered stochastic process ν that satisfies some mixing conditions that are needed in the asymptotic analysis and which are reviewed in for instance [1]. The typical example of such a process satisfying these mixing conditions will be an ergodic Markovian process that decorrelates exponentially fast.

$$\frac{1}{K(\mathbf{x}, z)} = \frac{1}{K(z)} = \left\{ \begin{array}{ll} \frac{1}{K}\left(1 + \nu(z/\varepsilon^2)\right) & \text{for} \quad z \in [0, L] \\ \frac{1}{K} & \text{for} \quad z \in (-\infty, 0) \cup (L, \infty) \end{array} \right.$$

$$\rho(\mathbf{x}, z) = \bar{\rho} \quad \text{for all} \quad (\mathbf{x}, z).$$

Below we show how the statistics of the propagating wave field derives from the statistics of ν. Observe that we model the medium as being layered or laminated, it only varies in the "depth" direction z. The random medium fluctuations are not small, they are $\mathcal{O}(1)$, and the fluctuations take place on the microscale, conveniently denoted by ε^2, where ε is a small parameter. In a number of physical problems the fluctuations in density is small compared to the fluctuations in the bulk modulus and for simplicity we take here the density to be constant. The general situation with fluctuations also in the density can be handled using a modification of the approach presented below. A point source is located in the homogeneous halfspace $z < 0$, we will give it explicitly in Section 2.

We are interested in how the medium fluctuations ν affects the propagating pulse. Consider first the case with a very long wave length for the propagating pulse, that is, a wavelength on the order of the propagation distance of size L.

Effective medium theory as discussed in [1] shows that then, to leading order, the wave propagates as if it where in an averaged or effective medium. The effective medium corresponds to replacing the reciprocal of the bulk modulus by its average value, $1/\overline{K}$, and also the density by its average value, which in this case is the constant density $\bar{\rho}$. Thus, we have centered the random medium fluctuations such that the pulse impinging from the halfspace $z < 0$ propagates as in a homogeneous medium and it is not affected by the random fluctuations ν. The parameters of the homogeneous halfspace matches those of the effective medium. However, if the wave length is short compared to the traveling distance then the random fluctuations ν will strongly affect the wave, this is the regime we consider here. More precisely we carry out our asymptotic analysis in the regime where the characteristic wavelength is $\mathcal{O}(\varepsilon)$, which is long compared to ε^2, the spatial scale of the random medium fluctuations are short compared to the distance of propagation, L, that we take to be $\mathcal{O}(1)$.

1.2. Time-reversal model problem. We describe the time-reversal model problem that we will analyze. The problem is illustrated in Figure 1.1 and involves the steps:

1. A point source is located in the halfspace $z < 0$ and generates an acoustic pulse that is impinging on the heterogeneous slab $0 < z < L$. The spatial width of the wave front that emanates from the source is **small** and $\mathcal{O}(\varepsilon)$. The wave field is subject to multiple scattering before it hits the time-reversal mirror, **TRM**, where it is recorded within a specific **time window**. Note that the TRM does not act as a usual mirror or strong reflector, but in a way that we now explain. We choose a narrow time window, of width $\mathcal{O}(\varepsilon)$, and located such that it records the wave front when it arrives at the TRM. We show below that this arrival time in the random case is approximately given by the arrival time in the effective medium. The spatial extent of the TRM in the transverse coordinates $\mathbf{x}$ is also chosen to be $\mathcal{O}(\varepsilon)$.

2. The pressure pulse that is captured in the given time window is **reversed** in time before it is re-emitted from the mirror and propagates toward the original source point. This means that the part of the signal that arrives last is re-emitted first.

3. Finally, we observe the wave front when it arrives back at the hyperplane $z = 0$ containing the original source point. The main issue we want to address is the spatial support of this re-propagated wave. If the TRM had recorded the transmitted wave for a long time and on a large spatial segment then the repropagated wave would be tightly focused at the original source point. Here, we consider the case with a small window, a small aperture, (ε/L), and we examine whether and how the repropagated wave focuses at the original source point. A key aspect in algorithms exploiting the time-reversal technique is exactly such tight re-focusing of the wave energy.

1.3. Summary of scales. Before we start the analysis of the problem we summarize the important scaling assumptions.

- The distance from the source point to the mirror is $L = \mathcal{O}(1)$.
- The magnitude of the random medium fluctuations are not small, they are $\mathcal{O}(1)$.
- The spatial scale at which the medium fluctuates is very small $\mathcal{O}(\varepsilon^2)$.
- The central wave length of the signal is small $\mathcal{O}(\varepsilon)$. Note that this is a scale in between the macro scale, $\mathcal{O}(L)$, and the micro scale, $\mathcal{O}(\varepsilon^2)$.
- The TRM is supported on the scale $\mathcal{O}(\varepsilon)$ in space and captures the wave front in a short time interval of width $\mathcal{O}(\varepsilon)$.
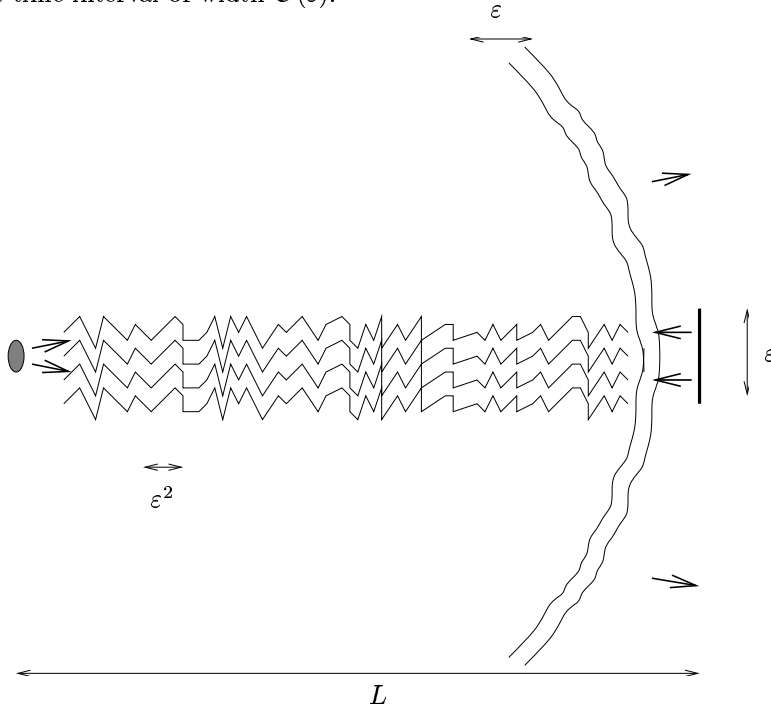

FIG. 1.1. *Setup*

2. The transmitted signal.

2.1. Plane wave representation. The analysis of the wave propagation problem described above is greatly simplified by the fact that the medium only varies in the depth z direction. It means that we can decompose the wave field into **plane wave** components

and analyze the propagation of each of these separately. Consider first a plane wave that is moving in the z direction in the homogeneous or effective medium with speed $\bar{c}$ and a characteristic wave-length $\mathcal{O}(\varepsilon)$, its pressure denoted by p_{hom} has the Fourier domain integral representation:

$$p_{hom}(t, \mathbf{x}, z) = f\left(\frac{t - z/\bar{c}}{\varepsilon}\right) = \frac{1}{2\pi} \int e^{-i\omega(t - z/\bar{c})/\varepsilon} \hat{f}(\omega) d\omega$$

$$= \frac{1}{2\pi} \int e^{-i\omega t/\varepsilon} \hat{f}(\omega) e^{i\omega z/(\varepsilon\bar{c})} d\omega$$

where the Fourier transform of the pulse shape is

$$\hat{f}(\omega) = \int e^{i\omega s} f(s) ds.$$

Consider next a plane wave that, relative to the spatial coordinates (x_1, x_2, z), is moving in the direction of the unit vector:

$$(\bar{c}\mathbf{k}, \sqrt{1 - \kappa^2 \bar{c}^2})$$

with the lateral slowness vector being

$$\mathbf{k} = (k_1, k_2)$$

and we denoted

(2.1) $$\kappa^2 = k_1^2 + k_2^2.$$

This oblique plane wave, propagating in the homogeneous medium, has the representation

(2.2) $$\frac{1}{2\pi} \int e^{-i\omega(t - \mathbf{k}\cdot\mathbf{x})/\varepsilon} \hat{f}(\omega) e^{i\omega z/(\varepsilon\bar{c}(\kappa))} d\omega$$

with the mode dependent speed in the z-direction being

(2.3) $$\bar{c}(\kappa) = \frac{\bar{c}}{\sqrt{1 - \kappa^2 \bar{c}^2}}.$$

We now exploit the fact that the medium does not depend on the transversal space variable $\mathbf{x}$ and decompose the problem into a family of problems involving such wave modes. First we eliminate the horizontal components of the velocity from (1.1)

(2.4) $$\rho \frac{\partial u}{\partial t} + \frac{\partial p}{\partial z} = 0$$

(2.5) $$\frac{1}{K(z)} \frac{\partial^2 p}{\partial t^2} - \frac{1}{\rho}\left(\frac{\partial^2 p}{\partial x_1^2} + \frac{\partial^2 p}{\partial x_2^2}\right) + \frac{\partial^2 u}{\partial z \partial t} = 0$$

with u being the velocity component in the z direction. It is convenient to take a joint Fourier transform in time and the lateral spatial dimensions (x_1, x_2). This joint transform decomposes the waves into plane wave modes according to (2.2):

$$\hat{u}^\varepsilon(\omega, \mathbf{k}, z) = \int\int\int e^{i\frac{\omega}{\varepsilon}(t - \mathbf{k}\cdot\mathbf{x})} u(t, \mathbf{x}, z) \, dt \, d\mathbf{x}$$

$$\hat{p}^\varepsilon(\omega, \mathbf{k}, z) = \int\int\int e^{i\frac{\omega}{\varepsilon}(t - \mathbf{k}\cdot\mathbf{x})} p(t, \mathbf{x}, z) \, dt \, d\mathbf{x}.$$

4

The inverse transform then becomes for instance for the pressure

$$p^\varepsilon(t, \mathbf{x}, z) = \frac{1}{(2\pi\varepsilon)^3} \int \int \int e^{-i\frac{\omega}{\varepsilon}(t - \mathbf{k} \cdot \mathbf{x})} \hat{p}^\varepsilon(\omega, \mathbf{k}, z) \omega^2 \, d\mathbf{k} \, d\omega.$$

Observe the presence of the factor ω^2 in this Fourier inverse due to our specific choice of Fourier variables. From (2.4) we obtain

$$-\frac{i\omega}{\varepsilon} \bar{\rho} \hat{u}^\varepsilon + \frac{\partial \hat{p}^\varepsilon}{\partial z} = 0$$
$$\frac{i\omega}{\varepsilon} \left(\frac{1}{K(z)} - \frac{\kappa^2}{\bar{\rho}} \right) \hat{p}^\varepsilon - \frac{\partial \hat{u}^\varepsilon}{\partial z} = 0$$

after factoring out an $i\omega$ in the second equation. Below we assume that the source is given such that we only need to consider non-evanescent modes corresponding to lateral slownesses (defined in (2.1)) satisfying $\kappa < C < 1/\bar{c}$ for some constant C. The speed of the modes are given by (2.3) and the **travel time** for mode $\mathbf{k}$ from the origin to depth z depends only on the lateral slowness $\kappa = |\mathbf{k}|$, it is

$$\tau(z, k) = z/\bar{c}(\kappa).$$

Similarly we define now the mode acoustic **impedance** by

$$\bar{I}(\kappa) = \bar{\rho}\bar{c}(\kappa).$$

With these definitions the equations for $\hat{p}^\varepsilon$ and $\hat{u}^\varepsilon$ can be written in the form

(2.6)
$$-\frac{i\omega}{\varepsilon} \bar{\rho} \hat{u}^\varepsilon + \frac{\partial \hat{p}^\varepsilon}{\partial z} = 0$$
$$-\frac{i\omega}{\varepsilon} \frac{1}{\bar{\rho}\bar{c}(\kappa)^2} \left(1 + \frac{\bar{c}(\kappa)^2}{\bar{c}^2} \nu(z/\varepsilon^2) \right) \hat{p}^\varepsilon + \frac{\partial \hat{u}^\varepsilon}{\partial z} = 0.$$

This shows that mode by mode the problem is a one-dimensional wave propagation problem. In fact, with κ fixed, this corresponds to a one dimensional wave propagation problem with density $\bar{\rho}$ and with the random **mode dependent** bulk modulus given by:

(2.7)
$$K_\kappa^{-1} = \frac{1}{\bar{\rho}\bar{c}(\kappa)^2} \left(1 + \frac{\bar{c}(\kappa)^2}{\bar{c}^2} \nu(z/\varepsilon^2) \right).$$

This is seen by performing a Fourier transform in time of the one-dimensional version of (1.1). We have therefore simplified the problem to a family of one-dimensional wave propagation problems.

2.2. One-dimensional mode problems. We now generalize the decomposition into right and left going waves to the non-homogeneous case. We decompose the solution of (2.6) into right and left going wave components for each plane wave mode by setting

(2.8)
$$\hat{p}^\varepsilon = \frac{\sqrt{\bar{I}(\kappa)}}{2} \left(\check{a}^\varepsilon e^{i\omega z/\varepsilon\bar{c}(\kappa)} - \check{b}^\varepsilon e^{-i\omega z/\varepsilon\bar{c}(\kappa)} \right)$$

(2.9)
$$\hat{u}^\varepsilon = \frac{1}{2\sqrt{\bar{I}(\kappa)}} \left(\check{a}^\varepsilon e^{i\omega z/\varepsilon\bar{c}(\kappa)} + \check{b}^\varepsilon e^{-i\omega z/\varepsilon\bar{c}(\kappa)} \right),$$

where $\check{a}^\varepsilon$ and $\check{b}^\varepsilon$ are unknown functions of ω, $\mathbf{k}$ and z. Outside the random slab this is an exact decomposition in the sense that these functions do not vary with z. We shall **retain**

5

this decomposition also in the slab $z \in (0, L)$ since it provides a centering with respect to the effective medium wave speed. We assume that a wave is impinging on the random slab from the left, giving the following boundary condition at $z = 0$:

$$(2.10) \qquad \qquad \check{a}^{\varepsilon}(\omega, \mathbf{k}, 0) = \varepsilon^2 \check{\phi}(\omega, \mathbf{k}).$$

We assume moreover that there is no energy coming in from the homogeneous halfspace $z > L$, which gives the second boundary condition at $z = L$:

$$(2.11) \qquad \qquad \check{b}^{\varepsilon}(\omega, \mathbf{k}, L) = 0.$$

The first condition gives in the Fourier domain the waves coming in from the homogeneous left halfspace $z < 0$. The particular form of $\check{\phi}$ depends on the particular choice of the physical source. For instance if $\check{\phi}$ is given by a pointmass at the mode $\mathbf{k}_0$ then the boundary condition corresponds to a time pulse oblique plane wave as above. The problem then reduces to a single one-dimensional problem of the type (2.6). In the following we consider more general functions $\check{\phi}$ which correspond to directed point sources, however, the particular form of $\check{\phi}$ is not important in our analysis. The multiplicative factor ε^2 derives from the fact that this is the particular scaling of the source magnitude that makes our quantity of interest $\mathcal{O}(1)$. Since the problem is linear this choice is however not important.

When we substitute the expressions (2.8) and (2.9) in (2.6) we get the following equations for the centered and transformed waves:

$$(2.12) \qquad \frac{d}{dz} \begin{bmatrix} \check{a} \\ \check{b} \end{bmatrix} = \frac{i\omega}{2\varepsilon \bar{c}(\kappa)} \nu_{\kappa} \left(z/\varepsilon^2 \right) \begin{bmatrix} 1 & -e^{-2i\omega z/\varepsilon \bar{c}} \\ e^{+2i\omega z/\varepsilon \bar{c}} & -1 \end{bmatrix} \begin{bmatrix} \check{a} \\ \check{b} \end{bmatrix}$$

where we defined

$$\nu_{\kappa}(z/\varepsilon^2) = \left(\frac{\bar{c}(\kappa)}{\bar{c}} \right)^2 \nu(z/\varepsilon^2).$$

Since the problem that we consider is a two point boundary value problem, rather than an initial value problem, we now introduce the propagators that satisfy:

$$(2.13) \qquad \frac{d}{dz} \mathbf{P}_{(\omega, \kappa)}^{\varepsilon}(0, z) = \frac{1}{\varepsilon} H_{(\omega, \kappa)} \left(z/\varepsilon, \nu_{\kappa}(z/\varepsilon^2) \right) \mathbf{P}_{\omega, \kappa}^{\varepsilon}(0, z)$$
$$\mathbf{P}_{(\omega, \kappa)}^{\varepsilon}(0, 0) = \mathbf{I}.$$

Observe that the propagator depends on the mode $\mathbf{k}$ only through $\kappa = \sqrt{k_1^2 + k_2^2}$. The matrix H depends on the fast variable z/ε through the phases and on the even faster variable z/ε^2 through the randomness ν:

$$H_{(\omega, \kappa)}(z, \nu_{\kappa}) = \frac{i\omega}{2\bar{c}(\kappa)} \nu_{\kappa} \begin{bmatrix} 1 & -e^{-2i\omega z/\bar{c}(\kappa)} \\ e^{+2i\omega z/\bar{c}(\kappa)} & -1 \end{bmatrix}.$$

From (2.13) it follows that we can express the propagator in the form:

$$\mathbf{P}_{\omega, \kappa}(0, L) = \begin{bmatrix} \alpha_{(\omega, \kappa)}^{\varepsilon}(0, L) & \overline{\beta_{(\omega, \kappa)}^{\varepsilon}(0, L)} \\ \beta_{(\omega, \kappa)}^{\varepsilon}(0, L) & \overline{\alpha_{(\omega, \kappa)}^{\varepsilon}(0, L)} \end{bmatrix}.$$

Since the trace of H is zero it also follows that

$$(2.14) \qquad \qquad |\alpha_{\omega}^{\varepsilon}|^2 - |\beta_{\omega}^{\varepsilon}|^2 = 1.$$

6

The transmitted right going wave is defined in terms of the harmonic amplitude $\breve{a}$ which solves:

$$\mathbf{P}_{(\omega,\kappa)}(0,L) \left[\begin{array}{c} \varepsilon^2 \breve{\phi}(\omega,\mathbf{k}) \\ \breve{b}(\omega,\mathbf{k},0) \end{array} \right] = \left[\begin{array}{c} \breve{a}(\omega,\mathbf{k},L) \\ 0 \end{array} \right],$$

therefore

$$(2.15) \qquad \breve{a}(\omega,\mathbf{k},L) = \frac{\varepsilon^2 \breve{\phi}(\omega,\mathbf{k})}{\alpha^{\varepsilon}_{(\omega,\kappa)}(0,L)}.$$

Using (2.14) we derive the important energy conservation relation:

$$(2.16) \qquad |\breve{a}(\omega,\mathbf{k},L)|^2 + |\breve{b}(\omega,\mathbf{k},0)|^2 = |\varepsilon^2 \breve{\phi}(\omega,\mathbf{k})|^2,$$

which in particular implies that the **transmission coefficient** $1/\overline{\alpha^{\varepsilon}_{(\omega,\kappa)}(0,L)}$ is uniformly bounded by one.

2.3. Integral representation for the transmitted wave. We now look at the right propagating transmitted wave within a time window centered at time t_0 and on the ε scale, that is, $A(t_0 + \varepsilon\sigma, \mathbf{x}, L)$. By Fourier inverse this quantity is given by

$$(2.17) \qquad A(t_0 + \varepsilon\sigma, \mathbf{x}, L)$$
$$= \frac{1}{(2\pi\varepsilon)^3} \int \int \int e^{-i\frac{\omega}{\varepsilon}(t_0 + \varepsilon\sigma - \mathbf{k}\cdot\mathbf{x} - L/\bar{c}(\kappa))} \breve{a}(\omega,\mathbf{k},L)\omega^2 d\mathbf{k} d\omega.$$

The expression (2.15) for the transmitted front wave mode gives then the following integral representation for the transmitted right-propagated wave component:

$$(2.18) \qquad A(t_0 + \varepsilon\sigma, \mathbf{x}, L)$$
$$= \frac{1}{(2\pi\varepsilon)^3} \int \int \int e^{-i\frac{\omega}{\varepsilon}(t_0 + \varepsilon\sigma - \mathbf{k}\cdot\mathbf{x} - L/\bar{c}(\kappa))} \frac{1}{\overline{\alpha^{\varepsilon}_{(\omega,\kappa)}(0,L)}} (\varepsilon^2 \breve{\phi}(\omega,\mathbf{k}))\omega^2 d\mathbf{k} d\omega.$$

Note that the corresponding expression for the pressure follows upon a scaling by $\sqrt{I(\kappa)}/2$ as can be easily seen from (2.8).

3. Review of O'Doherty-Anstey theory. Our objective is to understand time-reversal of transmitted waves. It is therefore essential to have a precise description of the transmitted wave front. We review here the theory that describes this front. The main result, the O'Doherty-Anstey formula, is presented in Section 3.3. Convergence of finite dimensional distributions for the front wave is derived in Section 3.1 using a moment argument as detailed in [7].

3.1. Characterization of moments. From the integral expression (2.18) we see that the transmission coefficients defined as $1/\overline{\alpha^{\varepsilon}_{(\omega,\kappa)}(0,L)}$ determine the transmitted wave field. From the energy-conservation (2.16) it follows that the modulus of this coefficient is bounded by one. It is important to note that the distribution of the wave in **time** and **space** depends on the **joint** distribution of the transformed wave over all frequencies ω and lateral wave-vectors $\mathbf{k}$. We next illustrate that knowledge of the joint moments of the transmitted wave for all **finite** combination of different frequencies and wave-vectors is enough to characterize the distribution of the transmitted wave in time and space. A convenient way to characterize

7

the finite dimensional distributions of the scalar wave is to compute the joint moments of order $m_1, \cdots, m_n$:

$$\mathbb{E}[A(t_{0,1} + \varepsilon\sigma_1, \mathbf{x}_1, L)^{m_1} \cdots A(t_{0,n} + \varepsilon\sigma_n, \mathbf{x}_n, L)^{m_n}],$$

which can be written in an integral form with respect to the variables $\omega_{j,l}, \mathbf{k}_{j,l}, \ 1 \le l \le n, \ 1 \le j \le m_l$:

$$\frac{1}{(2\pi\varepsilon)^{(3m)}} \int \cdots \int e^{-i\sum \omega_{j,l}\left(\sigma_l + \frac{\theta_{j,l}}{\varepsilon}\right)} \mathbb{E}\left[\prod \frac{1}{\alpha^{\varepsilon}_{(\omega_{j,l},\kappa_{j,l})}(0,L)}\right]$$
$$\times \left(\varepsilon^{2m} \prod \check{\phi}(\omega_{j,l}, \mathbf{k}_{j,l})\right) \prod \omega_{j,l}^2 d\mathbf{k}_{j,l} d\omega_{j,l},$$

where we defined

$$m = \sum_{l=1}^{n} m_l$$
$$\theta_{j,l} = \theta(t_{0,l}, \mathbf{k}_{j,l}, \mathbf{x}_l) = t_{0,l} - \mathbf{k}_{j,l} \cdot \mathbf{x}_l - L/\bar{c}(\kappa_{j,l})$$

and the sum and products are taken over all the distinct frequencies and wave-vectors. Therefore, we are led to study the joint distribution of the transmission coefficients

$$\frac{1}{\alpha^{\varepsilon}_{(\omega_j,\kappa_j)}(0,L)} = T^{\varepsilon}_{(\omega_j,\kappa_j)}(0,L)$$

for a finite number of frequencies and wave vectors. We now relabel these by $\omega_1, \cdots, \omega_m$ and $\mathbf{k}_1, \cdots, \mathbf{k}_m$. First, consider the situation with the phase $\theta_{j,l} = 0$. Then, if we can characterize the limits

(3.1) $$\lim_{\varepsilon \to 0} \mathbb{E}\left[T^{\varepsilon}_{(\omega_1,\kappa_1)}(0,L) \cdots T^{\varepsilon}_{(\omega_m,\kappa_m)}(0,L)\right]$$

of all these finite dimensional problems we would have characterized all the finite dimensional distributions of the transmitted wave front in space and time. It is shown in [7] for the one dimensional case and in [6] for the three dimensional layered case that the limit (3.1) is

(3.2) $$\mathbb{E}\left[\tilde{T}_{(\omega_1,\kappa_1)}(0,L) \cdots \tilde{T}_{(\omega_m,\kappa_m)}(0,L)\right]$$

where the coefficients $\tilde{T}$'s are solutions of the system of stochastic differential equations:

(3.3) $$d\tilde{T}_{(\omega_j,\kappa_j)} = -\omega_j^2 \frac{\gamma_{\kappa_j}}{2\bar{c}(\kappa_j)^2} \tilde{T}_{(\omega_j,\kappa_j)} dz + i\omega_j \frac{\sqrt{\gamma_{\kappa_j}}}{\bar{c}(\kappa_j)\sqrt{2}} \tilde{T}_{(\omega_j,\kappa_j)} dW(z)$$

driven by a **single** standard Brownian motion $W(z)$ and where the coefficient γ_κ is given by

(3.4) $$\gamma_\kappa = \int_0^\infty \mathbb{E}[\nu_\kappa(0)\nu_\kappa(s)]ds = \left(\frac{\bar{c}(\kappa)}{\bar{c}}\right)^4 \gamma$$

and

$$\gamma = \int_0^\infty \mathbb{E}[\nu(0)\nu(s)]ds.$$

8

The technique for deriving this result entail writing an expression for the multidimensional propagator that is associated with the frequencies and wave vectors $(\omega_j, \mathbf{k}_j)$. It satisfies an equation that generalizes the one in (2.13) for a single $\omega, \mathbf{k}$. Using a diffusion approximation result one can show that this multidimensional propagator converges in distribution to the solution of a multidimensional linear stochastic differential equation. Using Ito calculus one then derives stochastic differential equations that characterized the limiting transmission coefficients. One then takes expectations of the products of such coefficients and deduces that the limit is given by (3.2). Equation (3.3) admits the following explicit solution:

$$(3.5) \qquad \tilde{T}_{(\omega,\kappa)}(0, L) = \exp\left(i\omega \frac{\sqrt{\gamma_\kappa}}{\bar{c}(\kappa)\sqrt{2}} W(L) - \omega^2 \frac{\gamma_\kappa}{4\bar{c}(\kappa)^2} L \right),$$

as can be easily checked by applying Ito's formula. Therefore, if we substitute $1/\overline{\alpha}^\varepsilon$ for $\tilde{T}$ in (2.18) we obtain a characterization of the distribution for the wave front. This substitution leads to the correct asymptotic limit expression for the front also in the case with a fast phase, that is, when $\theta_{j,l}$ is non-zero. The small ε limit for the front is then obtained via a subsequent stationary phase argument, [6, 20], which gives the limit

$$(3.6) \qquad \tilde{a}(\sigma, \mathbf{x}, L) := (sp)\lim_{\varepsilon \to 0} A(t_0 + \varepsilon\sigma, \mathbf{x}, L)$$

$$= (sp)\lim_{\varepsilon \to 0} \frac{1}{(2\pi)^3 \varepsilon} \int\int\int e^{-i\omega\sigma} e^{-i\omega \frac{\theta(t_0, \mathbf{k}, \mathbf{x})}{\varepsilon}} \tilde{T}_{(\omega,\kappa)}(0, L) \check{\phi}(\omega, \mathbf{k}) \omega^2 d\mathbf{k} d\omega.$$

Observe that this integral expression has the exact scaling required for computing a two dimensional stationary phase limit and we compute this limit in the next section.

3.2. Stationary phase. The main contribution to the integral expression (3.6) occurs at the stationary point that solves:

$$\nabla_{\mathbf{k}}\theta = \begin{bmatrix} -x_1 - \dfrac{\partial}{\partial k_1}\left(\dfrac{L}{\bar{c}(\kappa)}\right) \\[2mm] -x_2 - \dfrac{\partial}{\partial k_2}\left(\dfrac{L}{\bar{c}(\kappa)}\right) \end{bmatrix} = \begin{bmatrix} -x_1 + Lk_1\bar{c}(\kappa) \\ -x_2 + Lk_2\bar{c}(\kappa) \end{bmatrix} = 0$$

which follows from (8.4.44) in [3]. It follows that the stationary lateral wave-vector, $\mathbf{k}_{sp}$, solves

$$(3.7) \qquad \mathbf{k}_{sp} = \frac{\bar{c}(\kappa_{sp})\mathbf{x}}{L} = \frac{\sqrt{1 - \bar{c}\kappa_{sp}^2 \mathbf{x}}}{\bar{c}L}$$

where we have used (2.3) and defined

$$\kappa_{sp}^2 = k_{sp,1}^2 + k_{sp,2}^2.$$

Solving (3.7) for κ_{sp}^2 we find

$$\bar{c}^2\kappa_{sp}^2 = \frac{|\mathbf{x}|^2}{|\mathbf{x}|^2 + L^2}.$$

We now substitute this explicit expression for $\bar{c}^2\kappa_{sp}^2$ into (3.7) to find the stationary point:

$$\mathbf{k}_{sp}(\mathbf{x}) = \frac{\mathbf{x}}{\bar{c}\sqrt{|\mathbf{x}|^2 + L^2}}.$$

9

We next substitute κ_{sp}^2 in (3.4) and obtain

$$\gamma_{\kappa_{sp}} = \left(\frac{1}{\sqrt{1 - \kappa_{sp}^2 \bar{c}^2}} \right)^4 \gamma = \left(1 + \frac{|\mathbf{x}|^2}{L^2} \right)^2 \gamma.$$

Finally, the value of the phase at the stationary point is given by

$$\theta(t_0, \mathbf{k}_{sp}, \mathbf{x}) = t_0 - \frac{\sqrt{|\mathbf{x}|^2 + L^2}}{\bar{c}},$$

and we choose t_0 to cancel it:

$$t_0 = \frac{\sqrt{|\mathbf{x}|^2 + L^2}}{\bar{c}}.$$

This corresponds to choosing t_0 to be the travel time from the source point at the origin to the point of observation $(\mathbf{x}, L)$ under the constant effective medium sound speed $\bar{c}$. We also have

$$\frac{\gamma_{\kappa_{sp}}}{\bar{c}(\kappa_{sp})^2} = \frac{\gamma}{\bar{c}^2} \left(1 + \frac{|\mathbf{x}|^2}{L^2} \right)$$

and upon substitution in (3.5) we find

$$\tilde{T}_{(\omega, \kappa_{sp})}(0, L) = \exp \left(i\omega \frac{\sqrt{\gamma}}{\bar{c}\sqrt{2}} \sqrt{1 + \frac{|\mathbf{x}|^2}{L^2}} \, W(L) - \omega^2 \frac{\gamma}{4\bar{c}^2} \left(1 + \frac{|\mathbf{x}|^2}{L^2} \right) L \right).$$

3.3. O'Doherty-Anstey formula. We have used the diffusion approximation limit to obtain a joint description of the plane wave modes and we next derive a simple explicit formula for the limit of the transmitted wave using the method of stationary phase. Applying the stationary phase result to (3.6) we find

$$\tilde{a}(\sigma, \mathbf{x}, L)$$
$$= \frac{1}{8\pi^2 \bar{c}^2 \sqrt{|\mathbf{x}|^2 + L^2}} \int e^{-i\omega\sigma} e^{i\omega \frac{\sqrt{\gamma}}{\bar{c}\sqrt{2}} \sqrt{1 + \frac{|\mathbf{x}|^2}{L^2}}} W(L) e^{-\omega^2 \frac{\gamma}{4\bar{c}^2} \left(1 + \frac{|\mathbf{x}|^2}{L^2} \right) L} i\omega \check{\phi}(\omega, \mathbf{k}_{sp}) d\omega.$$

The corresponding limit expression for the transmitted front $\tilde{a}_0$ in a constant medium is obtained by evaluating the above expression for $\gamma = 0$, we then find

$$\tilde{a}_0(\sigma, \mathbf{x}, L) = \frac{1}{8\pi^2 \bar{c}^2 \sqrt{|\mathbf{x}|^2 + L^2}} \int e^{-i\omega\sigma} i\omega \check{\phi}(\omega, \mathbf{k}_{sp}) d\omega.$$

This, then gives

THEOREM 3.1. *In probability distribution the following characterization of the transmitted wave process holds*

$$\lim_{\varepsilon \to 0} A \left(\frac{\sqrt{|\mathbf{x}|^2 + L^2}}{\bar{c}} + \varepsilon\sigma, \mathbf{x}, L \right) = \tilde{a}(\sigma, \mathbf{x}, L),$$

where

$$\tilde{a}(\sigma, \mathbf{x}, L) = \left[\tilde{a}_0(\cdot, \mathbf{x}, L) * \mathcal{N}_{D_{(L, \mathbf{x})}} \right] \left(\sigma - \theta_{(L, \mathbf{x})} \right)$$

10

and we denote

$$(3.8) \qquad D^2_{(L,\mathbf{x})} = \frac{\gamma}{2\bar{c}^2}\left(1 + \frac{|\mathbf{x}|^2}{L^2}\right)L$$

$$(3.9) \qquad \theta_{(L,\mathbf{x})} = \frac{\sqrt{\gamma\left(1 + \frac{|\mathbf{x}|^2}{L^2}\right)}}{\bar{c}\sqrt{2}}\, W(L)$$

$$\mathcal{N}_D(s) = \frac{1}{\sqrt{2\pi}D}e^{-s^2/2D^2}.$$

This result follows from the computations presented in sections 3.1 and 3.2 in the same manner as in [7] (one-dimensional case) and [6] (stationary phase limit). Observe that for L fixed only the random variable $W(L)$ is needed to characterize the probability distribution of the random field $\tilde{a}(\sigma, \mathbf{x}, L)$. Recall that $W(L)$ is a Gaussian random variable with mean zero and variance L. Note therefore that the shape of the front wave is given by the **deterministic** quantity

$$\tilde{a}_0(\cdot, \mathbf{x}, L) * \mathcal{N}_{D_{(L,\mathbf{x})}}.$$

This corresponds to a 'diffusion' in time or a smearing of the transmitted wave process via a convolution with the Gaussian function. This is often referred to as stabilization of the front and has also been obtained in [14, 20]. In the derivation presented there the shift by the Brownian motion $W(L)$ is handled by centering the front with respect to a random travel time. Thus, the front is observed in a frame that is random and depends on the particular realization of the random medium.

4. Time-reversal of transmitted front. We have discussed and characterized precisely the transmitted wave front and we can now start the mathematical analysis of the time-reversal problem that we presented in detail in Section 1.2. The time-reversal mirror (TRM) is defined by its support function in time and space. The time window on the ε scale is denoted by $G_1(\sigma)$ and the spatial extent in the ε scale by $G_2(\mathbf{x}')$,

$$G(\sigma, \mathbf{x}') = G_1(\sigma)G_2(\mathbf{x}').$$

This means that the signal recorded at the TRM is given by

$$y(\sigma, \mathbf{x}') = A(t'_0 + \varepsilon\sigma, \varepsilon\mathbf{x}', L)G_1(\sigma)G_2(\mathbf{x}')$$

where we have evaluated the transmitted field on the ε scale in time and space. Observe that this corresponds to looking at the transmitted signal on the micro or ε scale in a window centered at the time t_0 and around the position $(\mathbf{x} = 0, z = L)$. We find below that the appropriate choice for t'_0 is simply $t'_0 = L/\bar{c}$. This is a consequence of locating the TRM in an ε-neighborhood of $\mathbf{x} = 0$. In practice the TRM will be located in a neighborhood of some offset $\mathbf{x}_0$ this introduces a modification that we discuss in Section 4.6.

4.1. Time-reversed signal at the mirror. The time-reversed signal at the mirror is on the ε-scale given by

$$\psi(\sigma, \mathbf{x}') = y(-\sigma, \mathbf{x}') = A(t'_0 - \varepsilon\sigma, \varepsilon\mathbf{x}', L)G_1(-\sigma)G_2(\mathbf{x}').$$

In order to obtain a convenient integral expression for the wave field propagated **back** in the medium and evaluated at the original source plane we compute the specific Fourier transform

of the new source defined by ψ.

$$\hat{\psi}^\varepsilon(\omega, \mathbf{k}) = \int\int\int e^{i\omega(\sigma - \mathbf{k}\cdot\mathbf{x}')} A(t_0' - \varepsilon\sigma, \varepsilon\mathbf{x}', L) G_1(-\sigma) G_2(\mathbf{x}') d\sigma d\mathbf{x}'$$

$$= \int\int\int e^{i\omega(\sigma - \mathbf{k}\cdot\mathbf{x}')} \left\{ \frac{1}{(2\pi)^3\varepsilon} \int\int\int e^{-i\omega'(\sigma + \mathbf{k}'\cdot\mathbf{x}')} \overline{T^\varepsilon_{(\omega',\kappa')}(0,L)} \right.$$

$$\left. \times \overline{\check{\phi}(\omega', \mathbf{k}')} e^{i\frac{\omega'}{\varepsilon}\left(t_0' - L/\bar{c}(\kappa')\right)} \omega'^2 d\mathbf{k}' d\omega' \right\} G_1(-\sigma) G_2(\mathbf{x}') d\sigma d\mathbf{x}'$$

$$= \frac{1}{(2\pi)^3\varepsilon} \int\int\int \overline{T^\varepsilon_{(\omega',\kappa')}(0,L)}\,\overline{\check{\phi}(\omega', \mathbf{k}')}$$

$$\times \left\{ \int e^{i(\omega'-\omega)(-\sigma)} G_1(-\sigma) d\sigma \int\int e^{-i(\omega\mathbf{k} + \omega'\mathbf{k}')\cdot\mathbf{x}'} G_2(\mathbf{x}') d\mathbf{x}' \right\}$$

$$\times e^{i\frac{\omega'}{\varepsilon}\left(t_0' - L/\bar{c}(\kappa')\right)} \omega'^2 d\mathbf{k}' d\omega'$$

$$= \frac{1}{(2\pi)^3\varepsilon} \int\int\int \overline{T^\varepsilon_{(\omega',\kappa')}(0,L)}\,\overline{\check{\phi}(\omega', \mathbf{k}')}$$

(4.1)
$$\times \overline{\hat{G}_1(\omega - \omega')} \int\int e^{-i(\omega\mathbf{k} + \omega'\mathbf{k}')\cdot\mathbf{x}'} G_2(\mathbf{x}') d\mathbf{x}' e^{i\frac{\omega'}{\varepsilon}\left(t_0' - L/\bar{c}(\kappa')\right)} \omega'^2 d\mathbf{k}' d\omega'$$

where we used the fact that A is real.

4.2. The diffracted field. We observe the backpropagated or diffracted field at the plane $z = 0$, at the offset $\mathbf{x}$, and at the time $t_1 + \varepsilon\sigma$. This is our quantity of interest which we denote by S_L^ε and it is obtained by applying (2.18) to the new source $\hat{\psi}^\varepsilon$ given by (4.1):

$$S_L^\varepsilon(t_1 + \varepsilon\sigma, \mathbf{x}) = \frac{1}{(2\pi\varepsilon)^3} \int\int\int e^{-i\frac{\omega}{\varepsilon}(t_1 + \varepsilon\sigma - \mathbf{k}\cdot\mathbf{x} - L/\bar{c}(\kappa))} T^\varepsilon_{(\omega,\kappa)}(L,0)$$

$$\times \left\{ \varepsilon^2 \hat{\psi}^\varepsilon(\omega, \mathbf{k}) \right\} \omega^2 d\mathbf{k} d\omega$$

where $T^\varepsilon_{(\omega,\kappa)}(L,0)$ is the transmission coefficient from $z = L$ to $z = 0$. Observe that we **re-scale** the new source by the multiplicative factor ε^2 as in (2.18). This scaling takes into account the size of the TRM and is chosen such that our quantity of interest become $\mathcal{O}(1)$. Using the definition of the propagator in (2.13) we find that the transmission coefficient $T^\varepsilon_{(\omega,\kappa)}(L,0)$ satisfies

$$\mathbf{P}_{(\omega,\kappa)}(0,L) \begin{bmatrix} 0 \\ T^\varepsilon_{(\omega,\kappa)}(L,0) \end{bmatrix} = \begin{bmatrix} R^\varepsilon_{(\omega,\kappa)}(L,0) \\ 1 \end{bmatrix}$$

and therefore is given by

$$T^\varepsilon_{(\omega,\kappa)}(L,0) = \frac{1}{\overline{\alpha^\varepsilon_{\omega,\kappa}(0,L)}} = T^\varepsilon_{(\omega,\kappa)}(0,L).$$

After replacing $\hat{\psi}^\varepsilon(\omega, \mathbf{k})$ by its integral representation (4.1) we find

$$S_L^\varepsilon(t_1 + \varepsilon\sigma, \mathbf{x})$$

$$= \frac{1}{(2\pi)^6\varepsilon^2} \int\cdots\int e^{-i\omega\sigma} e^{-i\frac{\omega}{\varepsilon}(t_1 - \mathbf{k}\cdot\mathbf{x} - L/\bar{c}(\kappa))} e^{i\frac{\omega}{\varepsilon}(\mathbf{k}\cdot\mathbf{x})} e^{i\frac{\omega'}{\varepsilon}\left(t_0' - L/\bar{c}(\kappa')\right)}$$

$$\times \overline{\check{\phi}(\omega', \mathbf{k}')}\,\overline{\hat{G}_1(\omega - \omega')}\,\overline{T^\varepsilon_{(\omega',\kappa')}(0,L)}\,T^\varepsilon_{(\omega,\kappa)}(0,L)$$

$$\times \left\{ \int\int e^{-i(\omega\mathbf{k} + \omega'\mathbf{k}')\cdot\mathbf{x}'} G_2(\mathbf{x}') d\mathbf{x}' \right\} \omega'^2 \omega^2 d\mathbf{k}' d\omega' \, d\mathbf{k} d\omega.$$

A moment argument similar to the one given in Section 3.1 shows that the diffusion approximation limit is obtained by replacing the transmission coefficients T^ε by their corresponding coefficients $\breve{T}$ given explicitly in (3.5). It then remains to apply the stationary phase result to

$$\lim_{\varepsilon \to 0} S_L^\varepsilon (t_1 + \varepsilon\sigma, \mathbf{x})$$

$$= (sp) \lim_{\varepsilon \to 0} \frac{1}{(2\pi)^6 \varepsilon^2} \int \cdots \int e^{-i\omega\sigma} e^{-i\frac{\omega}{\varepsilon}(t_1 - \mathbf{k}\cdot\mathbf{x} - L/\bar{c}(\kappa))} e^{i\frac{\omega'}{\varepsilon}(t_0' - L/\bar{c}(\kappa'))}$$

$$\times \breve{\phi}(\omega', \mathbf{k}') \, \overline{\hat{G}_1(\omega - \omega')} e^{-i\omega' \frac{\sqrt{\gamma_\kappa}}{\bar{c}(\kappa')\sqrt{2}} W(L) - \omega'^2 \frac{\gamma_{\kappa'}}{4\bar{c}(\kappa')^2} L} e^{i\omega \frac{\sqrt{\gamma_\kappa}}{\bar{c}(\kappa)\sqrt{2}} W(L) - \omega^2 \frac{\gamma_\kappa}{4\bar{c}(\kappa)^2} L}$$

$$\times \left\{ \int\int e^{-i(\omega\mathbf{k} + \omega'\mathbf{k}')\cdot\mathbf{x}'} G_2(\mathbf{x}') d\mathbf{x}' \right\} \omega'^2 \omega^2 d\mathbf{k}' d\omega' \, d\mathbf{k} d\omega.$$

In the same manner as in Section 3.6 we can now apply the stationary phase theorem with respect to the two phases $t_1 - \mathbf{k}\cdot\mathbf{x} - L/\bar{c}(\kappa)$ and $t_0' - L/\bar{c}(\kappa')$. They give respectively the stationary points $\mathbf{k}_{sp}(\mathbf{x}) = \mathbf{x}/\bar{c}\sqrt{|\mathbf{x}|^2 + L^2}$ and $\kappa_{sp}' = 0$. The corresponding "stationary phase times" are $t_{(1,sp)} = \sqrt{|\mathbf{x}|^2 + L^2}/\bar{c}$ and $t_{(0,sp)} = L/\bar{c}$. We denote the limiting field by s_L and find

(4.2) $s_L(\sigma, \mathbf{x}) = \lim_{\varepsilon \to 0} S_L^\varepsilon (t_{(1,sp)} + \varepsilon\sigma, \mathbf{x})$

$$= \frac{-1}{16\pi^4 \bar{c}^4 L \sqrt{|\mathbf{x}|^2 + L^2}} \int\int e^{-i\omega\sigma} \overline{\breve{\phi}(\omega', \mathbf{0})} \, \overline{\hat{G}_1(\omega - \omega')} e^{-i(\omega'\theta_{(L,\mathbf{0})} - \omega\theta_{(L,\mathbf{x})})}$$

$$\times e^{-\omega'^2 D_{(L,\mathbf{0})}^2} e^{-\omega^2 D_{(L,\mathbf{x})}^2} \hat{G}_2(-\omega\mathbf{k}_{sp}) \omega\omega' d\omega d\omega'.$$

where we used the definitions (3.8) and (3.9) for quantities D_L^2 and θ.

4.3. Focusing functionals. If the TRM had covered the whole plane $z = L$ then the backpropagated wave would refocus tightly at the original source point, that is, $s_L(\sigma, \mathbf{x})$ would be supported near $\mathbf{x} = 0$. If the mirror is very small, as in our scaling, the refocusing becomes poor in the deterministic case. The fascinating phenomenon that we discuss next is that the random medium fluctuations give a refocused pulse also in the case with a very small aperture or spatial support of the TRM.

We now write the diffracted field (4.2) in terms of an integral of the initial time pulse by introducing a **focusing functional** $\mathcal{H}(s, \mathbf{x}; \sigma, L)$:

(4.3) $\quad s_L(\sigma, \mathbf{x}) = \frac{C}{r} \int \phi(s) \frac{(-1)}{4\pi^2} \int\int e^{-i(\omega's + \omega\sigma)} \overline{\hat{G}_1(\omega - \omega')} \hat{G}_2(-\omega\mathbf{k}_{sp})$

$$\times \left\{ e^{-i(\omega'\theta_{(L,\mathbf{0})} - \omega\theta_{(L,\mathbf{x})})} e^{-\omega'^2 D_{(L,\mathbf{0})}^2} e^{-\omega^2 D_{(L,\mathbf{x})}^2} \right\} \omega\omega' d\omega d\omega' ds$$

$$= \frac{C}{r} \int \phi(s) \mathcal{H}(s, \mathbf{x}; \sigma, L) ds$$

with $C = 1/(4\pi^2\bar{c}^4 L)$, $r^2 = |\mathbf{x}|^2 + L^2$ and where the time pulse ϕ is given by

$$\phi(s) = \frac{1}{2\pi} \int \overline{\breve{\phi}(\omega', \mathbf{0})} e^{i\omega's} ds.$$

In the deterministic case the term in the curly brackets in (4.3) is identically equal to one. In the random case this term plays a crucial role, it will enhance the decay in $\mathbf{x}$ of the focusing

13

functional $\mathcal{H}$. Note that if we denote by $\mathcal{H}_0$ the focusing functional in the deterministic case by

$$\mathcal{H}_0(s, \mathbf{x}; \sigma, L) = \frac{-1}{(2\pi)^2} \int \int e^{-i(\omega' s + \omega \sigma)} \overline{\hat{G}_1(\omega - \omega')} \hat{G}_2(-\omega \mathbf{k}_{sp}) \omega \omega' d\omega d\omega'$$

then in the random case it is given by

$$\mathcal{H}(s, \mathbf{x}; \sigma, L) = \mathcal{H}_0(s + \theta_{(L, \mathbf{0})}, \mathbf{x}; \sigma - \theta_{(L, \mathbf{x})}), L) *_s \mathcal{N}_{D_{(L, \mathbf{0})}} *_\sigma \mathcal{N}_{D_{(L, \mathbf{x})}}$$

where we differentiate between the commuting convolutions with respect to s and σ There-fore, the effect of the randomness in the medium can be described as introducing a new or effective focusing functional. It is obtained from the one in the deterministic case by convolution with deterministic Gaussian functions with respect to the time arguments and random shifts $\theta_{(L, \mathbf{x})}$ and $\theta_{(L, \mathbf{0})}$ in these arguments. As we show below, the fact that one of the Gaussian functions in the convolution has a $|\mathbf{x}|$ dependent width will give the focusing enhancement. By making the change of variables $\tilde{\omega} = \omega - \omega'$ and integrating with respect to $\tilde{\omega}$ we find

$$\mathcal{H}(s, \mathbf{x}; \sigma, L) = \frac{1}{2\pi} \int e^{-i\omega(\sigma + s)} \left[-iG_1'(s + \theta_{(L, \mathbf{0})}) - \omega G_1(s + \theta_{(L, \mathbf{0})}) \right] \hat{G}_2(-\omega \mathbf{k}_{sp})$$
$$\times \left\{ e^{-i\omega(\theta_{(L, \mathbf{0})} - \theta_{(L, \mathbf{x})})} e^{-\omega^2 D_{(L, \mathbf{x})}^2} \right\} \omega d\omega *_\sigma \mathcal{N}_{D_{(L, \mathbf{0})}}.$$

For simplicity we assume here that the mirror function $G_2(\mathbf{x})$ is rotationally invariant and relabel it $G_2(|\mathbf{x}|)$. When we then carry out the ω integration we find

$$\mathcal{H}(s, \mathbf{x}; \sigma, L) = \left[G_1'(s + \theta_{(L, \mathbf{0})}) \frac{\partial}{\partial s} + G_1(s + \theta_{(L, \mathbf{0})}) \frac{\partial^2}{\partial s^2} \right]$$
$$\times \int G_2 \left(\frac{-v}{\kappa_{sp}} \right) \frac{1}{\kappa_{sp}} \mathcal{N}_{D_{(L, \mathbf{x})}}(s + \sigma + \theta_{(L, \mathbf{0})} - \theta_{(L, \mathbf{x})} - v) dv *_\sigma \mathcal{N}_{D_{(L, \mathbf{0})}}.$$

Therefore, the random fluctuations in the medium corresponds to:

(i) An effective enhancement of the spatial support of G_2 through convolution with a Gaussian with variance given in (3.8).

(ii) A random displacement of the TRM given by

$$(4.4) \qquad \bar{\theta}_{(L, \mathbf{x})} := \theta_{(L, \mathbf{x})} - \theta_{(L, \mathbf{0})} = \frac{\sqrt{\gamma}}{\bar{c}\sqrt{2}} \left(\sqrt{1 + \frac{|\mathbf{x}|^2}{L^2}} - 1 \right) W(L)$$

where we have used (3.9).

4.4. Effective aperture. To obtain a more explicit characterization of the focusing we consider the case with the mirror being Gaussian in space and the identity in time:

$$G_1(s) = 1$$
$$G_2(v) = \mathcal{N}_a(v),$$

where the positive parameter a gives the size of the mirror (in the ε scale). Then we find

$$\mathcal{H}(s, \mathbf{x}; \sigma, L) = \frac{\partial^2 \mathcal{N}_{\Delta_{(L, \mathbf{x})}}(s + \sigma - \bar{\theta}_{(L, \mathbf{x})})}{\partial s^2}$$

14

with $\Delta_{(L,\mathbf{x})}$ being defined by

(4.5) $$\Delta^2_{(L,\mathbf{x})} = \kappa^2_{sp}a^2 + D^2_{(L,\mathbf{x})} + D^2_{(L,\mathbf{0})} = \kappa^2_{sp}a^2 + \frac{\gamma L}{2\bar{c}^2}\left(2 + \frac{|\mathbf{x}|^2}{L^2}\right).$$

We write this as

(4.6) $$\Delta^2_{(L,\mathbf{x})} = = \frac{\gamma L}{\bar{c}^2} + \kappa^2_{sp}a^2_{eff}$$

where we defined the **x** dependent **effective aperture**, or more precisely the effective sice of the mirror G_2, by

$$a^2_{eff} = a^2 + \frac{\gamma L}{2}\left(1 + \frac{|\mathbf{x}|^2}{L^2}\right).$$

From (4.3 we find that the wave field on the source plane is characterized by

$$s_L(\sigma, \mathbf{x}) = \frac{C}{r}\frac{\partial^2}{\partial\sigma^2}\int\phi(s)\,\mathcal{N}_{\Delta_{(L,\mathbf{x})}}(s + \sigma - \bar{\theta}_{(L,\mathbf{x})})ds.$$

Finally, it is convenient to consider the case with a Gaussian source pulse $\phi(s)$ with standard deviation denoted by T. In this case we define

(4.7) $$\bar{\Delta}^2_{(L,\mathbf{x})} := T^2 + \Delta^2_{(L,\mathbf{x})},$$

and write

$$s_L(\sigma, \mathbf{x}) = \frac{C}{r}\frac{\partial^2}{\partial\sigma^2}\mathcal{N}_{\bar{\Delta}_{(L,\mathbf{x})}}\left(\sigma - \bar{\theta}_{(L,\mathbf{x})}\right).$$

We look at the diffracted field at a given time, say a "snap-shot" at $\sigma = 0$, and by a simple explicit calculation we find

(4.8) $$s_L(0, \mathbf{x}) = \frac{C}{r}\frac{1}{\sqrt{2\pi}\bar{\Delta}^3_{(L,\mathbf{x})}}\left(-1 + \frac{\bar{\theta}^2_{(L,\mathbf{x})}}{\bar{\Delta}^2_{(L,\mathbf{x})}}\right)e^{-\bar{\theta}^2_{(L,\mathbf{x})}/\bar{\Delta}^2_{(L,\mathbf{x})}}.$$

The **diffraction field** in the homogeneous case is obtained by letting $\gamma = 0$. It is given explicitly by:

$$\frac{-C}{r\sqrt{2\pi}(T^2 + \kappa^2_{sp}a^2)^{3/2}}.$$

Recall that

$$\kappa_{sp} = \frac{|\mathbf{x}|}{\bar{c}r}$$
$$r^2 = |\mathbf{x}|^2 + L^2,$$

so that for large offsets $|\mathbf{x}|$ the amplitude of the diffracted field decays as $1/r$, that is as $1/|\mathbf{x}|$ for L fixed. This slow decay reflects the smallness of the mirror, it corresponds to the diffraction limit with the mirror effectively having point support in space. We contrast this decay with the decay in the random case when the diffracted field is given by (4.8). Observe that for $|\mathbf{x}|$ large we have

(4.9) $$\bar{\theta}^2_{(L,\mathbf{x})}/\bar{\Delta}^2_{(L,\mathbf{x})} \approx \frac{W(L)^2}{L}$$

15

which, in distribution, is the square of a standardized Gaussian random variable. The main difference from the homogeneous case is that in the random case (with $\gamma > 0$) $\bar{\Delta}_{(L,\mathbf{x})}$ is $\mathcal{O}(|\mathbf{x}|)$, and **not** $\mathcal{O}(1)$. Therefore, from (4.8), we find that the diffracted field decays as $1/|\mathbf{x}|^4$. Thus, we can conclude that in this sense the random medium gives a better refocusing (or "beats the diffraction limit").

4.5. Numerical illustration. From (4.8) and (4.9) we see that upon a normalization by the factor

$$\frac{C}{r} \frac{1}{\sqrt{2\pi}} \left(-1 + \frac{\bar{\theta}^2_{(L,\mathbf{x})}}{\bar{\Delta}^2_{(L,\mathbf{x})}} \right) e^{-\bar{\theta}^2_{(L,\mathbf{x})}/\bar{\Delta}^2_{(L,\mathbf{x})}}$$

the term $\bar{\Delta}^{-3}_{(L,\mathbf{x})}$ characterizes the lateral decay or the focusing of the diffracted field $s_L(0, \mathbf{x})$. It is convenient to rewrite $\bar{\Delta}^2_{(L,\mathbf{x})}$ in terms of nondimensionalized variables. From (4.6) and (4.7) we find:

$$\bar{\Delta}^2_{(L,\mathbf{x})} = T^2 \left(1 + \frac{a^2 |\mathbf{x}^2|}{r^2 \bar{c}^2 T^2} + \frac{\gamma L}{2\bar{c}^2 T^2} \left(2 + \frac{|\mathbf{x}|^2}{L^2} \right) \right).$$

We now introduce the wavelength $\lambda = \bar{c}T$ and we define the nondimensionalized variables

$$\tilde{a} = \frac{a}{\lambda}, \quad \tilde{x} = \frac{|\mathbf{x}|}{L}, \quad \tilde{\gamma} = \frac{\gamma L}{2\lambda^2}.$$

These quantities correspond respectively to the relative magnitudes of the aperture, the offset and the medium fluctuations. In terms of these variables the quantity of interest $\bar{\Delta}^{-3}_{(L,\mathbf{x})}$ can be written

$$\mathcal{F}(\bar{x}; \tilde{a}, \tilde{\gamma}) := T^3 \left(1 + \tilde{a}^2 \frac{\tilde{x}^2}{1 + \tilde{x}^2} + \tilde{\gamma}(2 + \tilde{x}^2) \right).$$

In order to compare the diffracted fields in the homogeneous and random cases we normalize $\mathcal{F}$ by its value at the origin. In Figure 4.1 we plot

$$\frac{\mathcal{F}(\tilde{x}; \tilde{a}, \tilde{\gamma})}{\mathcal{F}(0; \tilde{a}, \tilde{\gamma})}$$

for various parameter values.

- In the top plot we show the case with a narrow aperture, $\tilde{a} = 1/100$. The dotted, dashed and solid lines corresponds respectively to the deterministic, weak noise ($\tilde{\gamma} = 1/100$) and strong noise ($\tilde{\gamma} = 100$) cases. The dotted line shows that in the deterministic case there is no spatial focusing relative to the geometrical spreading of the deterministic medium, the mirror acts as a point source. However, random modulation in the medium creates focusing since wave energy 'traveling obliquely' relative to the layering is spread out relatively more due to the scattering.
- In the bottom plot we show the case with a wide aperture, with $\tilde{a} = 100$. In this case we have focusing also in the deterministic case, however, for large lateral offset the amplitude is still damped dramatically more in the random cases.

4.6. Generalization to the off-axis mirror case. The motivation for this generalization is that in the context of applications to imaging, the mirror might be located off the axis of the source. We find that the decay of wave energy with respect to the mirror
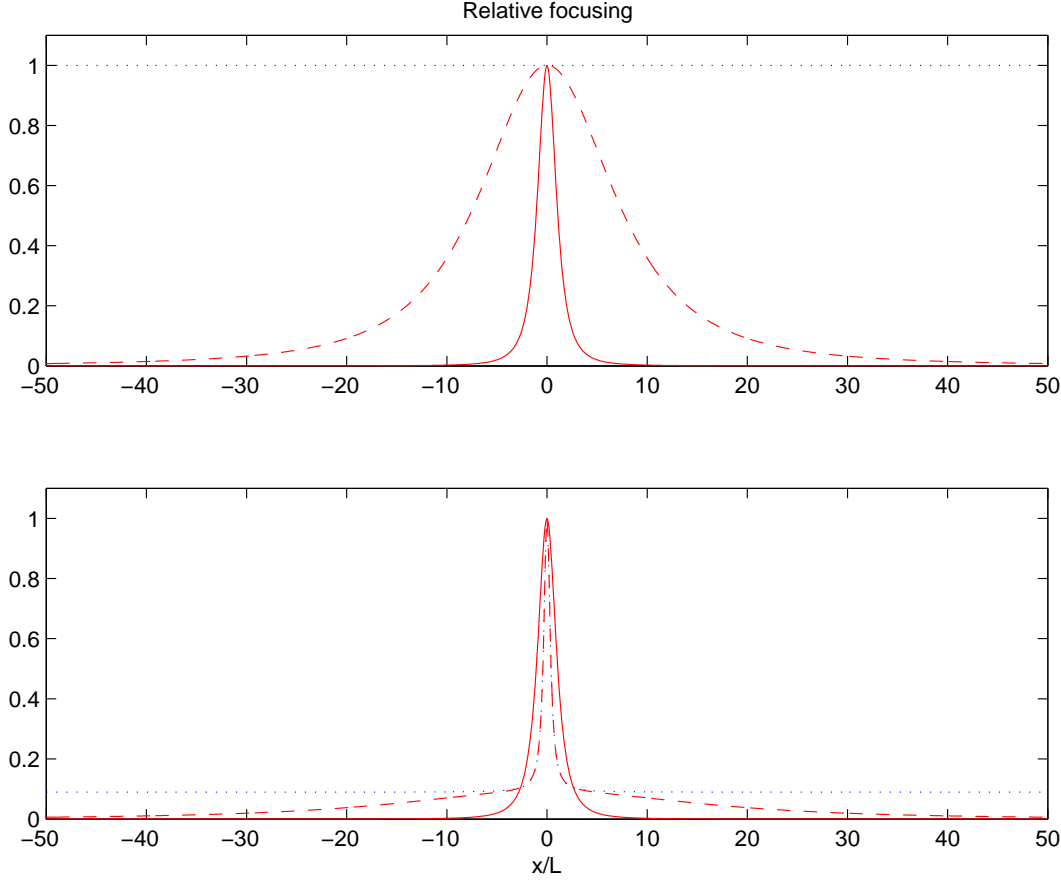
FIG. 4.1. *In this figures the dotted, dashed and solid lines correspond respectively to the homogeneous, weak noise and strong noise cases. The lines plot the relative focusing of the diffracted field as a function of the offset. The top figure illustrates the case with a narrow aperture where there is no focusing relative to the point source case for the homogeneous medium, while even in this regime randomness creates focusing. The bottom figure illustrates the case with a wide aperture where there is some focusing even in the homogeneous case. Note that in both cases the randomness in the medium improves the decay of the diffracted field.*

off-axis displacement is faster in the random case than in the homogeneous case. In this sense randomness improves the resolution in the source location problem.

We position the mirror off the axis of the source at the location $(\mathbf{d}, L)$. This means simply that we shift the mirror function G_2. In Section 4 $G_2(\mathbf{x}')$ is therefore replaced by $G_2(\mathbf{x}' - \mathbf{d}/\varepsilon)$ since G_2 is defined relative to the ε scale and the displacement of the mirror is $\mathcal{O}(1)$. When we make this modification and repeat the calculations in Section 4 we find that the diffracted field in (4.2) becomes:

$$s_L(\sigma, \mathbf{x}) = \frac{-1}{16\pi^4 \bar{c}^4 \sqrt{L^2 + |\mathbf{d}|^2} \sqrt{|\mathbf{x} - \mathbf{d}|^2 + L^2}} \int \int e^{-i\omega\sigma} \overline{\check{\phi}(\omega', \mathbf{0})} \, \overline{\hat{G}_1(\omega - \omega')}$$

$$\times e^{-i(\omega'\theta_{(L,\mathbf{d})} - \omega\theta_{(L,\mathbf{x}-\mathbf{d})})} e^{-\omega'^2 D^2_{(L,\mathbf{d})}} e^{-\omega^2 D^2_{(L,\mathbf{x}-\mathbf{d})}} \hat{G}_2(-\omega\mathbf{k}_{sp} - \omega'\mathbf{k}'_{sp}) \omega\omega' d\omega d\omega'.$$

17

where the modified stationary points are defined by

$$\mathbf{k}_{sp} = \frac{\mathbf{x} - \mathbf{d}}{\bar{c}\sqrt{(\mathbf{x} - \mathbf{d})^2 + L^2}}$$

$$\mathbf{k}'_{sp} = \frac{\mathbf{d}}{\bar{c}\sqrt{\mathbf{d}^2 + L^2}}.$$

Note that the times have been evaluated according to the stationary points as before. Following the analysis of Section 4.3 we find that the main effect of randomness is captured by the Gaussian exponentials

$$e^{-\omega'^2 D^2_{(L,\mathbf{d})}} e^{-\omega^2 D^2_{(L,\mathbf{x}-\mathbf{d})}}$$

which create fast decay with respect to the off-axis displacement $|\mathbf{d}|$.

5. Comments and conclusions. We have considered the phenomenon of super-resolution in the context of waves propagating from a point source in a randomly layered medium. In the regime of separation of scales we have obtained a precise description of the transmitted coherent field and also of the time reversed and backpropagated field, that is, the diffracted field. Our main interest has been in characterizing the spatial focusing properties of this diffracted field. We have shown that randomness improve the focusing. The reason for this improvement is a spreading in time of the coherent field. This spreading increases with the lateral offset from the source point. Observe that this is the mechanism that generates super-resolution, rather than multi-pathing effect, which is essential in the regime corresponding to the parabolic wave approximation, [4, 18]. In the layered case the random fluctuations in the medium creates randomness in the travel time of the coherent field and the main effect of time-reversal is to compensate for this random time shift. This is in contrast with the parabolic approximation regime where time-reversal is crucial in the refocusing enhancement.

In this paper we have considered only the **coherent** part of the wave field. In the regime that we consider with layered medium fluctuations strong incoherent wave components are generated by the scattering. These wave fluctuations can be observed in the coda of the transmitted field or in the incoherent reflected waves, this has been analyzed in [1]. Time-reversal of such incoherent waves is a very interesting problem. For the reflected field this has been considered in [8, 15, 19]. For applications to imaging and communication time-reversal of the transmitted incoherent field is important. The one-dimensional case with dispersive waves is studied in [10]. The general three dimensional layered case is the topic of a forthcoming paper.

REFERENCES

[1] M. Asch, W. Kohler, G. Papanicolaou, M. Postel, and B. White, Frequency content of randomly scattered signals, *SIAM Review* **33**, (1991) 519-626.
[2] G. Bal, G. Papanicolaou and L. Ryzhik, Self-averaging in time-reversal for the parabolic wave equation, to appear in Stochastics and Dynamics, (2002).
[3] N. Bleistein and R. A. Handelsman, Asymptotic Expansions of Integrals, Holt, Rinehart and Winston, (1975).
[4] P. Blomgren, G. Papanicolaou, and H. Zhao, Super-Resolution in Time-Reversal Acoustics, JASA, Vol 111, **Vol. 111**, (2002), pp. 230-248.
[5] B. Burridge, G. Papanicolaou, and B. White, Statistics for pulse reflexion from a randomly layered medium, *SIAM J. Appl. Math.*, **47**, (1987) 146-168.
[6] J. Chillan and J.P. Fouque, Pressure fields generated by acoustical pulses propagating in randomly layered media, *SIAM J. Appl. Math.* **58**, (1998) 1532-1546.

[7] J.F. Clouet and J.P. Fouque, Spreading of a pulse travelling in random media, *Annals of Applied Probability* **4**, (1994) 1083-1097.

[8] J.F. Clouet and J.P. Fouque A time-reversal method for an acoustical pulse propagating in randomly layered media, *Wave Motion* **25**, (1997) pp. 361-368.

[9] M. Fink, Time-reversed acoustics, *Scientific American,* November 1999, pp. 67-93.

[10] J.P. Fouque, J. Garnier and A. Nachbin, Time-reversal for dispersive waves in random media, preprint, 2002.

[11] J.P. Fouque, J. Garnier and A. Nachbin, The O'Doherty Anstey theory and time-reversal for nonlinear water waves in random media. preprint, 2002.

[12] J.P. Fouque and A. Nachbin, Time-reversed focusing of surface water waves, submitted 2002.

[13] P. Lewicki, R. Burridge and M. De Hoop, Beyond effective medium theory: pulse stabilization for multimode wave propagation in high-contrast layered media, *SIAM J. Appl. Math.* **56**, (1996) pp. 256-276.

[14] P. Lewicki, R. Burridge and G. Papanicolaou, Pulse stabilisation in a strongly heterogeneous layered medium, *Wave Motion* **20**, (1994) pp. 177-195.

[15] J. Ndzie, Refocusing of a time-reversed acoustical pulse propagating in randomly layered media, *J. Stat. Phys.*, Vol. 104, No. 516, (2001).

[16] A. Nachbin and K. Solna, Shallow water waves with a multiscale topography, submitted.

[17] R.F. O'Doherty and N.A. Anstey Refections on amplitudes, *Geophysical Prospecting* **19**, (1971) pp. 430-458.

[18] G. Papanicolaou, L. Ryzhik and K. Sølna, Statistical stability in time-reversal, (2002) submitted for publication.

[19] K. Sølna, Focusing of time-reversed reflections, accepted for publication in Waves in Random Media, (2002) .

[20] K. Sølna and G. Papanicolaou, Ray theory for a locally layered medium, Waves in Random Media, **10**, (2000) pp. 155-202.